

Optical and thermal performance of bladed receivers

John Pye, Joe Coventry, Clifford Ho, Julius Yellowhair, Ian Nock, Ye Wang, Ehsan Abbasi, Joshua Christian, Jesus Ortega, and Graham Hughes

Citation: [AIP Conference Proceedings](#) **1850**, 030040 (2017); doi: 10.1063/1.4984383

View online: <http://dx.doi.org/10.1063/1.4984383>

View Table of Contents: <http://aip.scitation.org/toc/apc/1850/1>

Published by the [American Institute of Physics](#)

Articles you may be interested in

[Development of ASTRI high-temperature solar receivers](#)

AIP Conference Proceedings **1850**, 030011 (2017); 10.1063/1.4984354

[A universal heliostat control system](#)

AIP Conference Proceedings **1850**, 030022 (2017); 10.1063/1.4984365

[SENER molten salt tower technology. Ouarzazate NOOR III case](#)

AIP Conference Proceedings **1850**, 030041 (2017); 10.1063/1.4984384

[Addressing forecast uncertainty impact on CSP annual performance](#)

AIP Conference Proceedings **1850**, 030015 (2017); 10.1063/1.4984358

[Novel imaging closed loop control strategy for heliostats](#)

AIP Conference Proceedings **1850**, 030005 (2017); 10.1063/1.4984348

[Towards high efficiency heliostat fields](#)

AIP Conference Proceedings **1850**, 030001 (2017); 10.1063/1.4984344



SUMMER SALE!

30% OFF
ALL PRINT
PROCEEDINGS!

AIP | Conference Proceedings

ENTER COUPON CODE
SUMMER2017

Optical and Thermal Performance of Bladed Receivers

John Pye^{1(a)}, Joe Coventry¹, Clifford Ho², Julius Yellowhair², Ian Nock¹, Ye Wang¹, Ehsan Abbasi¹, Joshua Christian², Jesus Ortega², and Graham Hughes³

¹ Solar Thermal Group, Research School of Engineering, Australian National University, Canberra, Australia

² Sandia National Laboratories, Albuquerque, USA

³ Imperial College, London, UK

^{a)}Corresponding author: john.pye@anu.edu.au

Abstract. Bladed receivers use conventional receiver tube-banks rearranged into bladed/finned structures, and offer better light trapping, reduced radiative and convective losses, and reduced tube mass, based on the presented optical and thermal analysis. Optimising for optical performance, deep blades emerge. Considering thermal losses leads to shallower blades. Horizontal blades perform better, in both windy and no-wind conditions, than vertical blades, at the scales considered so far. Air curtains offer options to further reduce convective losses; high flux on blade-tips is still a concern.

INTRODUCTION

Tubular receivers are dominant in almost all concentrating solar-thermal power (CSP) receivers in large-scale use. In central tower systems with significant storage, these receivers predominantly use molten salt as the working fluid. A constraint on these systems however is the peak flux limitation which, together with spillage and optical considerations, limits the minimum receiver area [1].

Bladed receivers are proposed as a concept to increase the efficiency of these tubular receivers, while maintaining low cost and using molten salt as the working fluid. Essentially, the banks of tubes taken from a convex cylindrical arrangement (such as in the Gemasolar or Crescent Dunes systems) are reconfigured into bladed or finned structures, thereby improving the light trapping performance and lowering radiative heat loss, while preserving a design based on long straight tubes and conventional materials (Figure 1). Bladed receivers as discussed here were proposed by Ho, Christian and Pye [2], although a similar concept (the ‘cruciform receiver’) was proposed by Vant-Hull [3]. A series of similar concepts have been developed independently by Wagner et al. at NREL [4] with an emphasis on direct heating of supercritical CO₂.

This paper examines bladed receiver performance with emphasis on molten salt applications. A first-order model is followed by more detailed results from optical ray-tracing, and radiative and convective heat loss models.

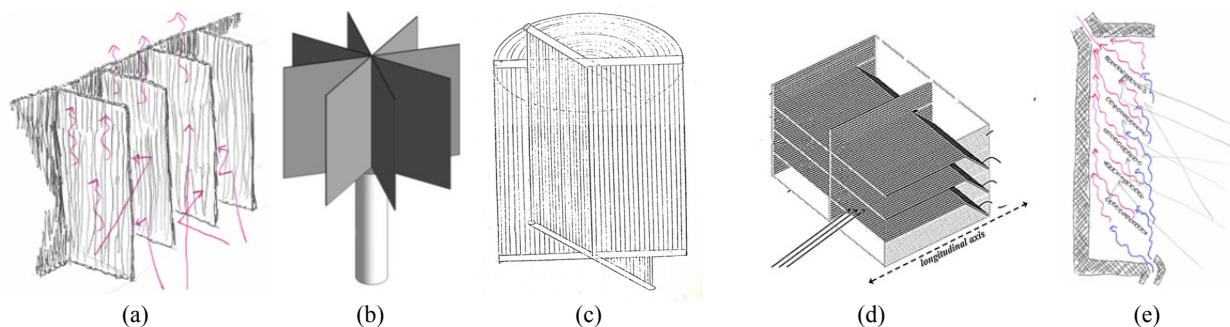


FIGURE 1. Concepts for bladed receivers: (a) vertical bladed receiver panels, (b) ‘star’ receiver configuration [2], (c) ‘cruciform’ receiver [3], (d) ‘bookshelf’ receiver [4], and (e) ‘louvred’ bladed receiver with active airflow control.

MOTIVATION AND FIRST-ORDER MODEL

Overcoming the flux limits on molten salt receivers is a core motivation for the development of the bladed receiver concept. Falcone [1] notes that different working fluids have different characteristic flux limits: for water, it is around 600 suns; for molten salt, around 850–1000 suns; for sodium, around 1300–1750 suns. Limitations arise due to thermal stresses, creep, corrosion and cyclical fatigue, as well as stability limits on the working fluid (around 600°C for molten salt) [1]. Peak flux limitations are more challenging in the hottest parts of a receiver, since excessive flux can too easily cause tube or working fluid temperatures to be exceeded [5]. Current molten salt receivers operating near these various flux limits typically achieve a receiver efficiency of the order of 90% [1, 5].

The dominant heat loss mechanisms for high temperature tubular receivers are reflection and re-radiation. For defined working fluid limits, the heat loss is essentially proportional to the receiver aperture area (although somewhat non-linear, since higher flux causes increased external wall temperatures). Hence, an option to increase receiver efficiency beyond 90% is to increase the concentration ratio and decrease the receiver aperture.

A bladed receiver addresses the challenge of maintaining tube peak-flux within limits while reducing the aperture by taking a flat/convex receiver operating at its flux limit and ‘folding up’ its tube banks into a smaller aperture (Figure 2). A simple geometric analysis demonstrates the first-order behaviour of bladed receivers compared to flat receivers. If the receiver height is H , and the width across the receiver is covered with N blades with spacing S , and the blade depth (out-of-plane from H and S) is B , then the external (irradiated) surface area of the tube-banks may be approximated (for N large) as

$$A = N(2B + S)H \quad (1)$$

The mass of the tubes in the receiver, on the other hand, is

$$m = N(B + S)H\rho' \quad (2)$$

where ρ' is the mass per area of tube bank. Note the factor of two in Eq. 1, which reflects the fact that tubes are irradiated on both sides. The ratio of bladed receiver mass to irradiated area is

$$\frac{m}{A} = \frac{N(B + S)H\rho'}{N(2B + S)H} = \frac{(B + S)}{(2B + S)}\rho' = \left(\frac{\frac{B}{S} + 1}{2\frac{B}{S} + 1}\right)\rho' < \rho' \quad (3)$$

So we see that bladed receivers require a lower mass of tubes for an equal irradiated tube-bank area compared to a flat receiver (where $m/A = \rho'$), and this ratio depends only on the blade length to spacing ratio $R_{BS} = B/S$, and not on the number of blades. Tube-bank frontal areas are considered here; the effect of crevices between tubes is ignored but could be incorporated through use of a modified tube-bank absorptivity/emissivity.

Next, we estimate the net absorbed energy for a bladed receiver, with blades assumed vertical, compared to a flat receiver. We assume that both receivers have the same total incident irradiance, uniformly distributed over the receiver surfaces, and we assume that the irradiated tube area A for both receivers is equal. For this analysis we will make use of the result for the effective emissivity ϵ_{eff} of a diffuse grey isothermal cavity with aperture area A_{ap} , internal cavity area A and internal surface emissivity ϵ , from Holman [6]:

$$\frac{\epsilon_{\text{eff}}}{\epsilon} = \frac{1}{(A_{\text{ap}}/A)(1 - \epsilon) + \epsilon} \quad (4)$$

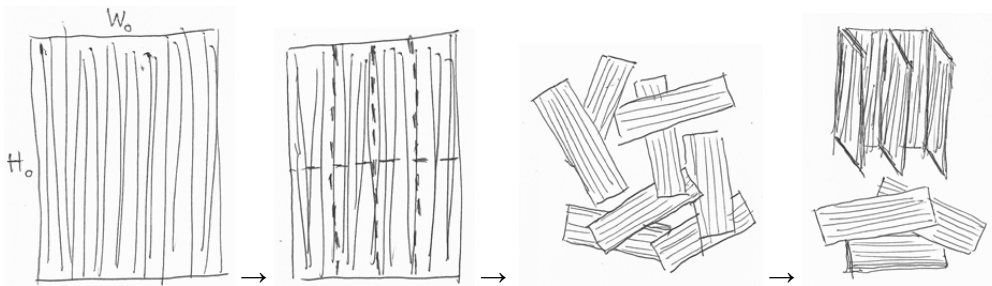


FIGURE 2. Conceptually, a bladed receiver with an equal irradiated area can be constructed by taking apart and reassembling tube-banks from a conventional convex receiver. A lower mass of tubes is required to reach the desired area, because the blade portions are double-sided. On the assumption that an equal total irradiance could be uniformly distributed on the bladed configuration, both the mass and receiver losses would be reduced, while the peak flux limitation is still respected.

For the flat receiver, the incident irradiance is $\dot{Q}_{\text{inc}} = GCA$ where G is the direct normal irradiance, C is the average concentration ratio for the solar field at selected operating conditions and A is the flat receiver area. The absorbed irradiance, with $\alpha = \varepsilon = (1 - \rho)$ (noting the relation between absorptance α , emissivity ε , and reflectance ρ), is $\dot{Q}_{\text{abs}} = \varepsilon\dot{Q}_{\text{inc}}$. The thermal emission losses can be calculated on the assumption that the receiver temperature $T \gg T_{\text{amb}}$, hence $\dot{Q}_{\text{emit}} = \varepsilon A \sigma T^4$, where σ is the Stefan-Boltzmann constant. The net energy absorbed is then

$$\dot{Q}_{\text{net,flat}} = \varepsilon A (GC - \sigma T^4). \quad (5)$$

Meanwhile, the bladed receiver will have a reduced aperture $A_{\text{ap}} = NSH$ (hence $A_{\text{ap}}/A = S/(2B + S)$), increased effective emissivity (Eq. 4), and increased concentration on its aperture C' , giving

$$\dot{Q}_{\text{net,bladed}} = \varepsilon_{\text{eff}} A_{\text{ap}} (GC' - \sigma T^4). \quad (6)$$

If the total incident irradiance is equal for both receivers then $GC'A_{\text{ap}} = GCA$ and Eq 6 becomes

$$\dot{Q}_{\text{net,bladed}} = \frac{\varepsilon_{\text{eff}}}{\varepsilon} \varepsilon A \left(GC - \frac{A_{\text{ap}}}{A} \sigma T^4 \right) = \frac{\varepsilon_{\text{eff}}}{\varepsilon} \dot{Q}_{\text{net,flat}} + \varepsilon_{\text{eff}} \sigma T^4 [A - A_{\text{ap}}] \quad (7)$$

Hence we see that the net energy absorbed for the bladed receiver has increased relative to the flat receiver through two mechanisms: firstly, the cavity effect increases the net absorbed energy according to $\varepsilon_{\text{eff}}/\varepsilon$; secondly, energy losses associated with the larger-aperture flat receiver, $\varepsilon_{\text{eff}} \sigma T^4 (A - A_{\text{ap}})$ are eliminated and this energy is absorbed instead.

These relationships are plotted in Figure 3 starting with a flat $10 \times 10 \text{ m}^2$ flat receiver with $C=800$ and $G=1000 \text{ W/m}^2$, tube diameter $D_o=70 \text{ mm}$, tube thickness $t=4 \text{ mm}$, tube density $\rho=8000 \text{ kg/m}^3$ and tube emissivity 0.94. Blades are added with increasing blade depth-to-spacing ratio $R_{BS} = B/S$ (initially zero) always preserving constant total incident irradiance and irradiated tube area A . As blades deepen, the receiver aperture concentration ratio increases, the receiver mass decreases significantly, and the receiver efficiency $\eta = \dot{Q}_{\text{net}}/GCA$ increases towards one, but the average flux on the tubes remains constant.

This analysis shows that if uniform flux can be achieved through careful arrangement of the blades into a smaller aperture, then receivers can potentially be designed which are simultaneously lighter, more efficient, but still respecting the tube peak flux limits. Achieving a smaller aperture (higher concentration) implies higher requirements from the heliostat field, a requirement that will not be discussed here. Achieving uniform flux on the blades seems very challenging, however, and will be discussed in the next section. Although motivated by molten salt, the benefits of bladed receivers as outlined here are equally applicable to other working fluids, such as supercritical CO_2 .

OPTICAL PERFORMANCE

The first-order analysis of bladed receivers above included an assumption of uniform flux over the entire receiver surface, but experience even with flat receivers shows that this is impossible in practice. It is necessary to understand how well the potential benefits of bladed receivers can be retained while at the same time looking at and managing more realistic flux profiles. Ho et al. [7] modelled the optics of a ‘star’ configuration (Figure 7),

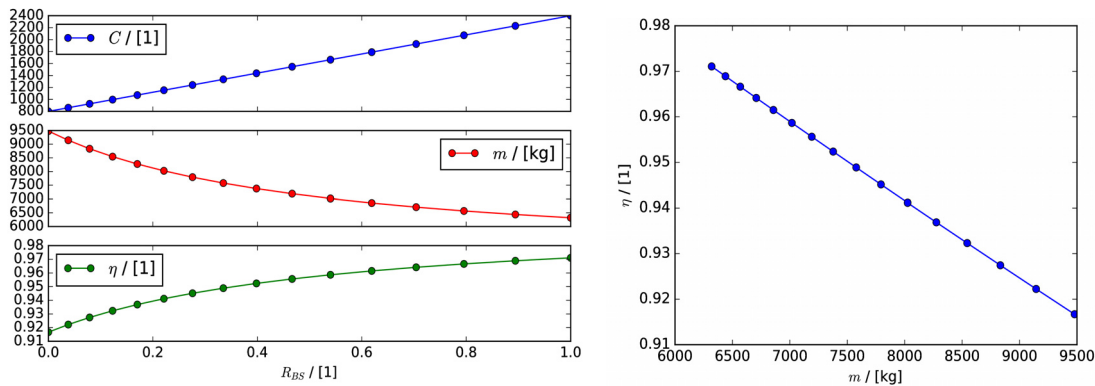


FIGURE 3. First-order evaluation of a bladed receiver sized on the assumption of uniform flux at the tube surface and with total irradiance constant held constant. Left: as longer blades are used (blade depth-to-spacing ratio R_{BS} increases), the concentration ratio increases linearly. Interestingly, there is a negatively-sloped linear relationship between the receiver efficiency η and the receiver mass m : double-side receiver panel allow the bladed receiver to be lighter than the flat receiver.

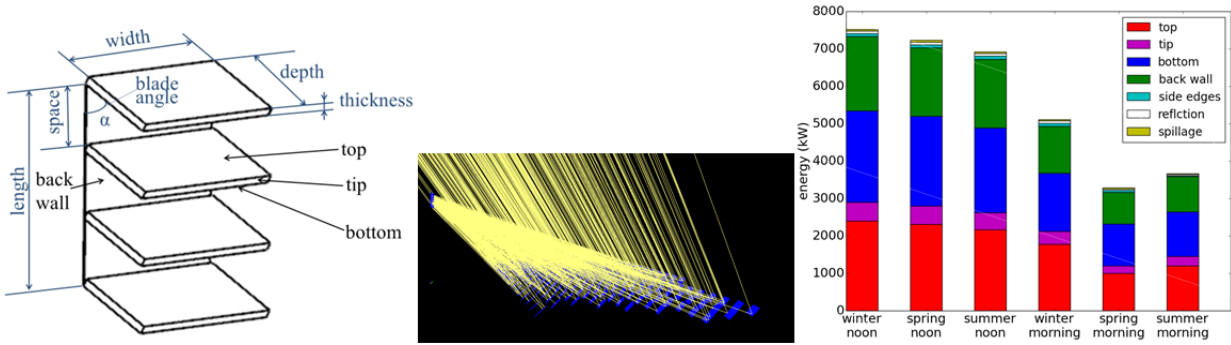


FIGURE 4. Results from ray tracing of the Sandia NSTTF solar field with a horizontal bladed receiver (centre). Blade depth, spacing and angle (left) were varied and optimised for optical efficiency at equinox noon. The receiver achieves ~98% optical efficiency for all sun positions considered, with ~4-5% lower losses than a flat receiver of the same back-wall size. For the optimal design, energy is relatively evenly distributed on the upper and lower blade surfaces (right).

highlighting the difficulties of attaining an even flux distribution. A significant concern is the flux on the blade tips, which, due to the curved wall of the tubes, will unavoidably have at least some surfaces oriented in the unfavourable directions for blade tip flux. Nevertheless, there are numerous geometric parameters that can be varied, including blade depth-to-spacing ratio R_{BS} , blade orientation (horizontal, vertical, ‘star’), blade angle α (especially for horizontal blades, the angle of the blade relative to vertical), and the aiming strategy of the heliostat field (for example, aiming at the tip of the blades or at the back wall).

Looking specifically at horizontal blades, Wang et al. [8] undertook an optimisation of the geometry (Figure 4) considering only optical efficiency $\eta_{opt} = \dot{Q}_{abs}/(\dot{Q}_{inc} + \dot{Q}_{spil})$, where \dot{Q}_{spil} is the spilled portion of the concentrated solar flux directed towards the receiver. Ray tracing was conducted in Python using the open-source *Tracer* code, and optimisation was conducted for equinox noon only. The optimal configuration was found to have very long blades

($B = 4.5$ m, $R_{BS} \approx 7$) inclined $\alpha = 63.9^\circ$ from vertical, an angle almost exactly parallel with the line from the centre of the back-wall to the middle of the heliostat field. Flat heliostats were assumed, as an approximation and were all aimed at the back-wall centre. Although this makes the focal-region fluxes lower than realistic, the angular distribution of incident radiation from the heliostat field remains quite realistic, so the optimum is believed to be robust. Tube banks were also approximated as planar, ignoring, for now, the effects of the tube circular cross-section. Peak flux on the back-wall, blade-tip and blade top/bottom surfaces were 60, 48 and 19 kW/m² respectively, compared to 171 kW/m² for a flat receiver. The performance of the optimal configuration at other sun positions was examined, and the observed high optical efficiency of the receiver was found to be surprisingly insensitive to sun position. The shares of total energy absorbed on back-wall, tops and bottoms of blades (taken together) was roughly equal (Figure 4 right). For these very long blades and with focus at the back-wall, peak flux was found to occur at the back-wall, not at the blade tips.

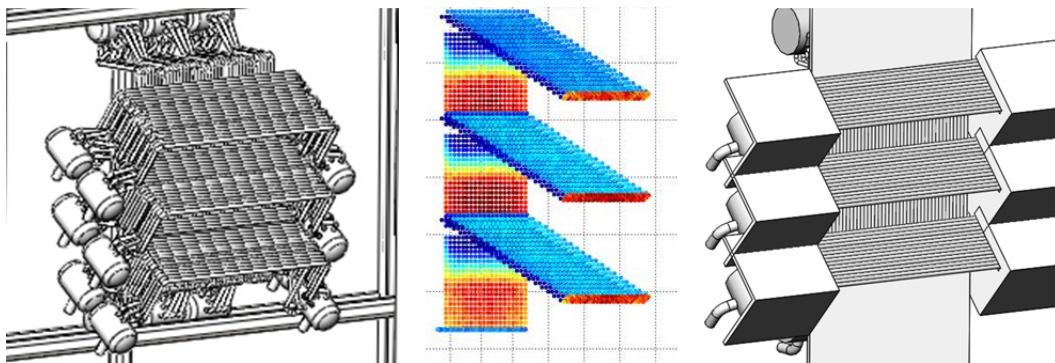


FIGURE 5. Left, the proposed supercritical CO₂ experimental bladed receiver set-up of Christian et al [9]. Centre, ray-tracing analysis shows high flux on the blade tips in this design ($R_{BS} \approx 1.4$), which are proposed to be replaced by a ceramic material instead of metal tubes. Right, cowling to cover the blade-end manifolds and associated equipment has been arranged to avoid overly obscuring the back-wall from lateral flux.

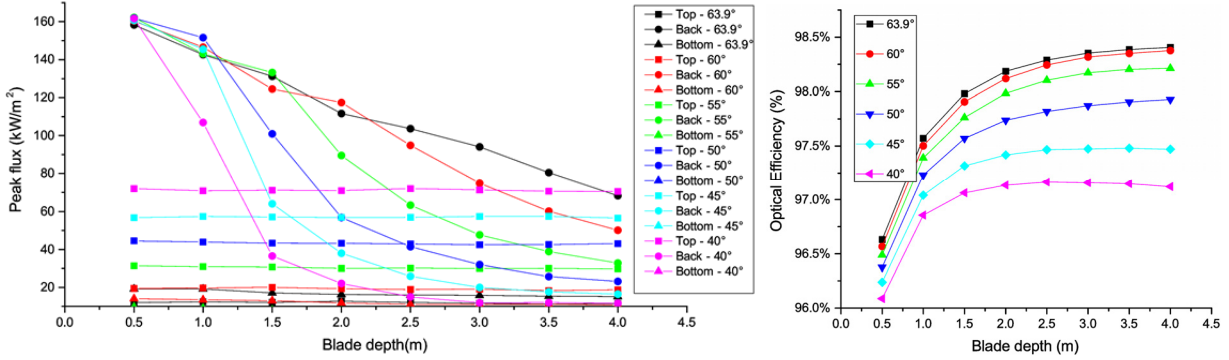


FIGURE 6. Blade performance as a function of blade depth and blade angle, with blade spacing 0.63 m: left, peak flux; right, optical efficiency. Results are based on the Sandia NSTTF solar field, modelled with flat heliostats. Although the flux values are not representative, it is expected that the relative changes are accurate: increasing the blade depth significantly reduces the peak flux on blades, and further reduction is possible by tilting the blades more steeply (smaller angle α). Only a small reduction in receiver efficiency occurs as a result of modifying the design to respect peak flux limits.

The long $R_{BS} \approx 7$ blades above demonstrate excellent optical performance, but the long blades it is highly doubtful that such long blades would be feasible in practice; either cost or thermal losses will lead to optimal designs with shorter blades. Furthermore, although peak flux was reduced to almost one third, the distribution of flux is highly non-uniform. Successfully reducing the mass of the receiver while increasing the focal-plane concentration, as described in §0, depends on uniform flux. However, the optically-optimal long blades of Wang et al. [8] will significantly *increase* the mass of the receiver if peak flux limits are to be respected (the opposite trend to that of Eq. 3). Figure 6 presents the results of further analysis, using the same model, and shows the influence of blade angle for various blade depths. Tilting the blades down from the angle of peak optical efficiency allows the irradiance to be more evenly shared by the blades, and peak flux reduces more sharply with shorter blades, with only modest reduction of optical efficiency. This inspires concepts with blade length and tilt tailored to the optical characteristics of the heliostat field, including receivers with varying blade length, and is the subject of further work.

Christian et al. [9] conducted another study of the geometric parameters of bladed receivers. From a set of 297 configurations, they selected a preferred design achieving effective solar absorptance $\alpha_{eff} = \dot{Q}_{abs}/\dot{Q}_{inc}$ of 96.6%, with a blade angle $\alpha=50^\circ$ and $R_{BS} \approx 1.4$. This design also uses the back-wall as the focal plane for the heliostat field. They will proceed to build and test this new receiver on the Sandia NSTTF solar field in 2016 (Figure 5).

As noted earlier, peak flux is typically not seen at the blade tip when the focal plane is at the back-wall, however as blades become shorter there will be a cross-over beyond which peak flux will occur at the tips, and in an optimised design it may even be necessary to replace active tubes at the blade tip with a passive ceramic component better able to survive the high fluxes. Christian et al. propose to conduct their testing with these ceramic ‘dummy’ tubes to avoid the risk of tube failure. This will naturally reduce receiver performance slightly, but is an important consideration for receiver reliability.

DESIGN TO MINIMISE RADIATIVE HEAT LOSS

The bladed receiver concept can improve upon the performance predicted by the first-order model (above) in one import aspect. Since the receiver is used to heat up a working fluid, it is expected that receiver external temperatures will vary over a similar temperature range to that of the working fluid. At the same time, the cavity-like geometry between the blades means that local radiative view factors from the blade surface to the surroundings vary significantly: high at the blade tips, and relatively low on the ‘interior’ surfaces such as the back-wall. The flow path in a bladed receiver is therefore configured so that cold fluid travels from the blade tip to towards the interior.

This configuration of cool tips, hot interiors is common to a range of high-efficiency receiver concepts, including this ANU/Sandia concept [2] (lateral tubes), the NREL concept [4] (longitudinal tubes) as well as the ‘pyramid’ receiver of Garbrecht et al [10] and the spiky ‘SCRAP’ receiver of Lubkoll et al [11], and is also the object of the ‘volumetric effect’ sought after for open air receivers, where flow also takes a longitudinal path, and where outer surfaces are expected to have lower temperatures than the inner surfaces, yielding lower radiative heat loss [12, 13].

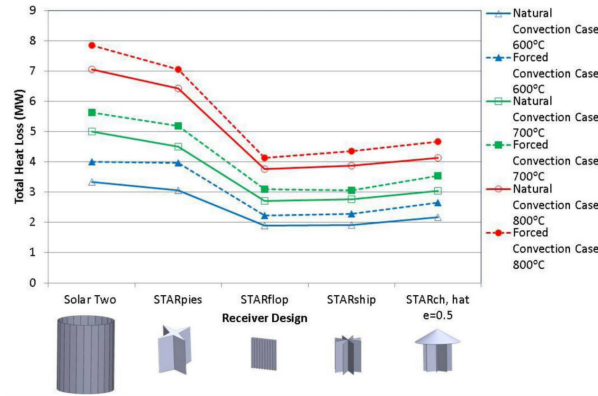


FIGURE 7. Natural and forced (7 m/s, horizontal) convection plus radiative heat loss from a range of bladed receivers at different (uniform) surface temperatures. All cases have an equal surface area of 100 m². For the ‘STARflop’ flat bladed receiver, wind is normal to the aperture plane [7].

NATURAL AND FORCED CONVECTION HEAT LOSS

In the first-order model (above0), convective losses were neglected. The bladed configuration, however, is likely to interrupt and ‘trip’ boundary layer flows over its surface, and it is possible that a bladed receiver may experience significantly higher convective heat losses, since although A_{ap} is considerably smaller, wetted area A is unchanged.

Ho et al. [7] previously conducted computational fluid dynamics (CFD) modelling of natural and forced convection heat loss from sample bladed receivers including ‘star’ and vertical bladed configurations (Figure 1), but did not consider the case of horizontal blades. On an assumption of equal irradiated area and uniform surface temperature, the vertical bladed receiver was found to have the lowest natural convection losses (Figure 7). The modelled receiver scale was ~ 100 m²; steady-state solutions with ~ 1 M cells and the $k-k_L-\omega$ turbulence model.

More recent work by Christian et al. [14] examined natural convection heat loss on smaller 4 m² receiver modules using *SolTrace* and a multi-aim-point strategy to establish flux boundary conditions, and included heat-sink wall boundary conditions. A discrete ordinates (DO) radiation model for radiative heat loss and $k-\omega$ SST turbulence model were used with Fluent. Horizontal blades showed the best performance, mostly because of slightly better radiative performance than the vertical blades. Wind was not considered.

Horizontal blades are expected to provide reduced convective heat loss compared to vertical blades because of the trapped stratified region that occurs underneath inclined blades, especially in no-wind conditions, but it is not yet clear how well horizontal blades would perform in windy conditions.

New CFD models developed here re-examine the effect of wind on bladed receivers, with vertical and horizontal configurations considered. The receiver considered is a small 50×50 cm bladed receiver (sized for compatibility with wind-tunnel validation currently in progress) with $R_{BS}=3$ with perpendicular blades, and receiver aperture inclined at 26° to the vertical. A non-uniform temperature distribution is assumed, from 310°C at the blade tips, to 585°C at the blade stem, and uniform 585°C across the back-wall. Tube-banks are approximated as flat, and the total wetted ‘hot’ area is 1.72 m². The problem is solved with the OpenFOAM *buoyantSimpleFoam* solver and $k-\omega$ SST turbulence model, and mesh invariance has been established. The viscous sub-layer is resolved down to $y^+ < 3$. Zero-wind (1.8M cells), 1 m/s and 2 m/s winds (both 2.5M cells) are selected on the basis of the wind speeds expected to show mixed convection behaviour according to standard empirical correlations. Results (Figure 8) show that as expected, horizontal blades perform better in no-wind conditions. However the horizontal bladed configuration also performs better in mixed convection (1 m/s) and moderately forced convection (2 m/s) conditions at this scale. The lower heat loss for horizontal blades is understood to occur because horizontal wind gives flows that are more generally aligned with the receiver surfaces, allowing larger boundary layers to build up. There are only isolated cases where vertical blades outperform horizontal blades: wind from the rear, and strong head-on wind. Sample flow patterns (Figure 9) are indicated by isothermal surfaces ($T=102^\circ\text{C}$) surrounding the hot receiver surface.

Due to boundary layer behaviour and the tendency for partial stratification underneath blades, it is thought that horizontal blades are preferable to vertical blades in the case of convection, but results to date have been limited to small scale, and scaling effects may need to be considered.

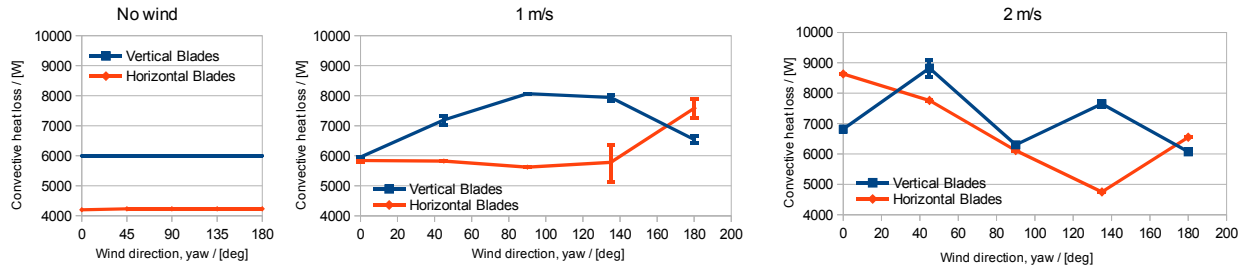


FIGURE 8. Variation in receiver heat loss from vertical and horizontal bladed receivers at 310–585°C, with a 0.5×0.5 m back plane, for no wind, as well as wind from various directions at 1 and 2 m/s. For natural convection and low wind, losses from horizontal blades are seen to be significantly lower for most wind directions. At higher wind speeds, the losses for horizontal blades start to increase. Low wind speeds were selected to approximate the mixed convection regime expected at larger scales.

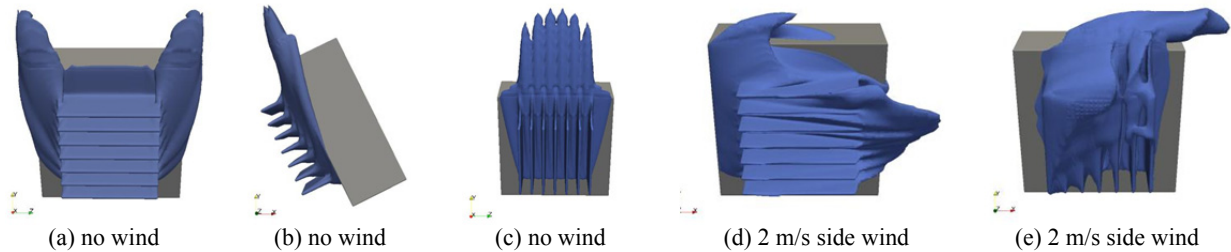


FIGURE 9. Examples of the flow structure around vertical and horizontal bladed receivers; blue surfaces indicated the limit of the air $T > 102^\circ\text{C}$ region; receiver surface temperatures were varied between 310°C at tips and 585°C across the back-wall. Note that, following §0, receiver are tilted downwards towards the assumed centre of the heliostat field.

ACTIVE AIRFLOW FEATURES

Previous work with cavity cavities [15-18] and convex central tower receivers [19] has highlighted the potential reduction (~40%) in convective heat loss which can be achieved through the use of air jets and air curtains, especially in no-wind conditions. It is less clear whether active airflow features can cost-effectively reduce heat loss for a receiver during windy conditions. Air curtains and related concepts are being considered for use with bladed receivers. A challenge for an air curtain on a large cavity-like receiver is that very large amounts of air must be blown across the aperture in order to ‘seal’ its convective heat loss. Instead, it may be possible to inject air at the tip of each receiver blade, potentially via the ceramic ‘dummy’ tubes mentioned earlier. Figure 10 shows a number of ‘blade-tip air jet’ concepts currently under evaluation. Combined air extraction, recuperation (heat recovery through a heat exchanger) and re-injection is also being considered as a potential approach to reduce convective heat loss. The effect of wind on these air curtains is also of concern, and numerical and experimental investigations are ongoing.

CONCLUSIONS

Bladed receivers have been shown to offer significantly higher receiver efficiency for molten salt tubular receivers, without requiring a change in the working temperature range, by overcoming the peak-flux limitation inherent in convex receiver designs. Convective heat loss modelling suggests that horizontal blades may be

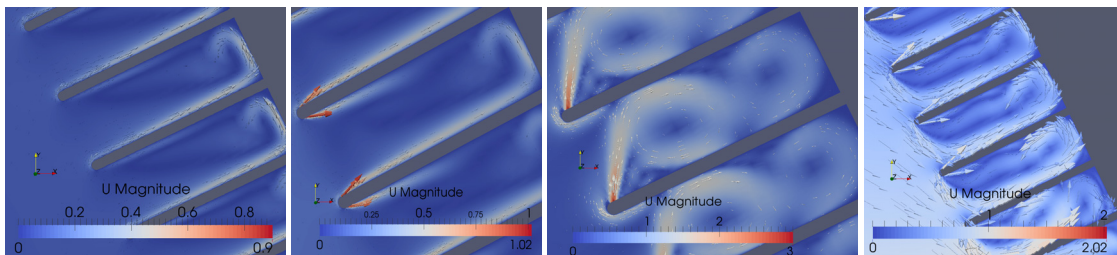


FIGURE 10. Blade-tip air-jet concepts. From left: bladed receiver with still air, no jet; still air, 1 m/s jet at 20° to the blade surface; still air, vertical air jet at 3 m/s; head-wind at 1 m/s and jets at 20°.

preferably to vertical blades in most wind and no-wind conditions. Optical modelling has established some feasible configurations that achieve high optical efficiency without exceeding allowable flux, however further work on peak flux limits especially on the blade tips is required. Air curtains and other active airflow control mechanisms are considered for potential further reductions in bladed receiver heat loss.

ACKNOWLEDGEMENTS

This work was supported by the Australian Renewable Energy Agency, grant 2014/RND010. Sandia National Laboratories is a multi-program laboratory managed and operated by Sandia Corporation, a wholly owned subsidiary of Lockheed Martin Corporation, for the U.S. Department of Energy's National Nuclear Security Administration under contract DE-AC04-94AL85000. The United States Government retains and the publisher, by accepting the article for publication, acknowledges that the United States Government retains a non-exclusive, paid-up, irrevocable, world-wide license to publish or reproduce the published form of this manuscript, or allow others to do so, for United States Government purposes.

REFERENCES

1. P. K. Falcone (1986). A handbook for Solar Central Receiver Design, Sandia Report SAND86-8009, Sandia National Laboratories, Albuquerque, NM.
2. C. K. Ho, J. M. Christian and J. D. Pye (2014). 'Bladed solar thermal receivers for concentrating solar power', United States Provisional Patent No. 14/535,100 (filed 8 November 2013).
3. L. L. Vant-Hull, C. R. Applebaugh, J. P. Colaco, C. Easton, S. Gronich, R. W. Hallet, A. Hildebrandt, F. Lipps, R. McFee, J. Raetz and W. Rigdon (1974). Solar thermal power systems based on optical transmission (a feasibility study), Semi-annual progress report to the US National Science Foundation NSF/RANN/SE/GI-39456/PR/73/4, University of Houston and McDonnell Douglas Astronautics West, Houston, Texas.
4. M. Wagner, Z. Ma, J. Martinek, T. Neises and C. Turchi (2014). 'Systems and methods for direct thermal receivers using near blackbody configurations', United States Provisional Patent No. 61/993,671 (filed 15 May 2014).
5. G. J. Kolb (2011). An Evaluation of Possible Next-Generation High-Temperature Molten-Salt Power Towers, Sandia Report SAND2011-9320, Sandia National Laboratories, Albuquerque.
6. J. P. Holman, 2009. *Heat transfer*. McGraw-Hill.
7. C. K. Ho, J. M. Christian, J. D. Ortega, J. Yellowhair, M. J. Mosquera and C. E. Andraka (2014). Reduction of radiative heat losses for solar thermal receivers. In *Proceedings of the SPIE Optics+Photonics Solar Energy+Technology High and Low Concentrator Systems for Solar Energy Applications IX*, San Diego, CA.
8. Y. Wang, C.-A. Asselineau, J. Coventry and J. Pye (2016). Optical performance of bladed receivers for CSP systems. In *Proceedings of the ASME 2016 Power and Energy Conference*, Charlotte, North Carolina.
9. J. M. Christian, J. D. Ortega, C. K. Ho and J. Yellowhair (2016). Design and modelling of light-trapping tubular receiver panels. In *Proceedings of the ASME 2016 10th International Conference on Energy Sustainability*, Charlotte, North Carolina.
10. O. Garbrecht, F. Al-Sibai, R. Kneer and K. Wieghardt (2013). *Sol. Energy* **90**, 94-106.
11. M. Lubkoll, T. von Backström, T. Harms and D. Kröger (2015). *Energy Procedia* **69**, 461-470.
12. M. Romero, R. Buck and J. E. Pacheco (2002). *J. Sol. Energy Eng.* **124**, 98-108.
13. A. L. Ávila-Marín (2011). *Solar Energy* **85**, 891-910.
14. J. M. Christian, J. D. Ortega and C. K. Ho (2015). Novel tubular receiver panel configurations for increased efficiency of high-temperature solar receivers. In *Proceedings of the ASME 2015 9th International Conference on Energy Sustainability*, San Diego, California.
15. A. McIntosh, G. Hughes and J. Pye (2014). Use of an air curtain to reduce heat loss from an inclined open-ended cavity. In *Proceedings of 19th Australasian Fluid Mechanics Conference*, Melbourne, Australia.
16. G. Hughes, J. Pye, M. Kaufer, E. Abbasi-Shavazi, J. Zhang, A. McIntosh and T. Lindley (2015). Reduction of Convective Losses in Solar Cavity Receivers. In *Proceedings of SolarPACES 2015*, Capetown, South Africa.
17. J. J. Zhang, J. D. Pye and G. O. Hughes (2015). Active air flow control to reduce cavity receiver losses. In *ASME Power & Energy 2015*.
18. R. Flesch, J. Grobbel, H. Stadler, R. Uhlig and B. Hoffschmidt (2016). *AIP Conference Proceedings* **1734**.
19. R. T. Taussig (1984). Aerowindows for central solar receivers. In *ASME Winter Annual Meeting*, New Orleans